

# Plasmonic analog of electromagnetically induced transparency in nanostructure graphene

Xi Shi,<sup>1</sup> Dezhuan Han,<sup>1,2</sup> Yunyun Dai,<sup>1</sup> Zongfu Yu,<sup>3,5</sup> Yong Sun,<sup>4</sup>  
Hong Chen,<sup>4</sup> Xiaohan Liu,<sup>1</sup> and Jian Zi<sup>1,\*</sup>

<sup>1</sup>Department of Physics, Key Laboratory of Micro & Nano Photonic Structures (MOE), and Key Laboratory of Surface Physics, Fudan University, Shanghai 200433, China

<sup>2</sup>Department of Applied Physics, College of Physics, Chongqing University, Chongqing 400044, China

<sup>3</sup>College of Engineering, University of Wisconsin–Madison, Madison, WI 53706, USA

<sup>4</sup>Pohl Institute of Solid State Physics, Tongji University, Shanghai 200092, China

<sup>5</sup>zyu54@wisc.edu

\*jzi@fudan.edu.cn

**Abstract:** Graphene has shown intriguing optical properties as a new class of plasmonic material in the terahertz regime. In particular, plasmonic modes in graphene nanostructures can be confined to a spatial size that is hundreds of times smaller than their corresponding wavelengths in vacuum. Here, we show numerically that by designing graphene nanostructures in such deep-subwavelength scales, one can obtain plasmonic modes with the desired radiative properties such as radiative and dark modes. By placing the radiative and dark modes in the vicinity of each other, we further demonstrate electromagnetically induced transparency (EIT), analogous to the atomic EIT. At the transparent window, there exist very large group delays, one order of magnitude larger than those offered by metal structures. The EIT spectrum can be further tuned electrically by applying a gate voltage. Our results suggest that the demonstrated EIT based on graphene plasmonics may offer new possibilities for applications in photonics.

©2013 Optical Society of America

OCIS codes: (050.6624) Subwavelength structures; (230.4555) Coupled resonators.

---

## References and links

1. Q. Xu, S. Sandhu, M. L. Povinelli, J. Shakya, S. Fan, and M. Lipson, “Experimental realization of an on-chip all-optical analogue to electromagnetically induced transparency,” *Phys. Rev. Lett.* **96**(12), 123901 (2006).
2. N. Papasimakis, V. A. Fedotov, N. I. Zheludev, and S. L. Prosvirnin, “Metamaterial analog of electromagnetically induced transparency,” *Phys. Rev. Lett.* **101**(25), 253903 (2008).
3. S. Zhang, D. A. Genov, Y. Wang, M. Liu, and X. Zhang, “Plasmon-induced transparency in metamaterials,” *Phys. Rev. Lett.* **101**(4), 047401 (2008).
4. X. Yang, M. Yu, D.-L. Kwong, and C. W. Wong, “All-optical analog to electromagnetically induced transparency in multiple coupled photonic crystal cavities,” *Phys. Rev. Lett.* **102**(17), 173902 (2009).
5. P. Tassin, L. Zhang, T. Koschny, E. N. Economou, and C. M. Soukoulis, “Low-loss metamaterials based on classical electromagnetically induced transparency,” *Phys. Rev. Lett.* **102**(5), 053901 (2009).
6. Y. Sun, H. Jiang, Y. Yang, Y. Zhang, H. Chen, and S. Zhu, “Electromagnetically induced transparency in metamaterials: Influence of intrinsic loss and dynamic evolution,” *Phys. Rev. B* **83**(19), 195140 (2011).
7. T. Zentgraf, S. Zhang, R. F. Oulton, and X. Zhang, “Ultrathin coupling-induced transparency bands in hybrid plasmonic systems,” *Phys. Rev. B* **80**(19), 195415 (2009).
8. N. Liu, L. Langguth, T. Weiss, J. Kästel, M. Fleischhauer, T. Pfau, and H. Giessen, “Plasmonic analogue of electromagnetically induced transparency at the Drude damping limit,” *Nat. Mater.* **8**(9), 758–762 (2009).
9. R. D. Kekatpure, E. S. Barnard, W. Cai, and M. L. Brongersma, “Phase-coupled plasmon-induced transparency,” *Phys. Rev. Lett.* **104**(24), 243902 (2010).
10. L. Verslegers, Z. Yu, Z. Ruan, P. B. Catrysse, and S. Fan, “From electromagnetically induced transparency to superscattering with a single structure: a coupled-mode theory for doubly resonant structures,” *Phys. Rev. Lett.* **108**(8), 083902 (2012).
11. A. H. Castro Neto, F. Guinea, N. M. R. Peres, K. S. Novoselov, and A. K. Geim, “The electronic properties of graphene,” *Rev. Mod. Phys.* **81**(1), 109–162 (2009).
12. B. Wunsch, T. Stauber, F. Sols, and F. Guinea, “Dynamical polarization of graphene at finite doping,” *New J. Phys.* **8**(12), 318 (2006).

13. E. H. Hwang and S. Das Sarma, "Dielectric function, screening, and plasmons in two-dimensional graphene," *Phys. Rev. B* **75**(20), 205418 (2007).
14. M. Jablan, H. Buljan, and M. Soljačić, "Plasmonics in graphene at infrared frequencies," *Phys. Rev. B* **80**(24), 245435 (2009).
15. F. Bonaccorso, Z. Sun, T. Hasan, and A. C. Ferrari, "Graphene photonics and optoelectronics," *Nat. Photonics* **4**(9), 611–622 (2010).
16. A. N. Griorenko, M. Polini, and K. S. Novoselov, "Graphene plasmonics," *Nat. Photonics* **6**(11), 749–758 (2012).
17. F. Wang, Y. Zhang, C. Tian, C. Girit, A. Zettl, M. Crommie, and Y. R. Shen, "Gate-variable optical transitions in graphene," *Science* **320**(5873), 206–209 (2008).
18. L. Ju, B. Geng, J. Horng, C. Girit, M. Martin, Z. Hao, H. A. Bechtel, X. Liang, A. Zettl, Y. R. Shen, and F. Wang, "Graphene plasmonics for tunable terahertz metamaterials," *Nat. Nanotechnol.* **6**(10), 630–634 (2011).
19. F. H. Koppens, D. E. Chang, and F. J. Garcia de Abajo, "Graphene plasmonics: a platform for strong light-matter interactions," *Nano Lett.* **11**(8), 3370–3377 (2011).
20. A. Yu Nikitin, F. Guinea, F. J. Garcia-Vidal, and L. Martín-Moreno, "Edge and waveguide terahertz surface plasmon modes in graphene microribbons," *Phys. Rev. B* **84**(16), 161407 (2011).
21. J. Gu, R. Singh, X. Liu, X. Zhang, Y. Ma, S. Zhang, S. A. Maier, Z. Tian, A. K. Azad, H.-T. Chen, A. J. Taylor, J. Han, and W. Zhang, "Active control of electromagnetically induced transparency analogue in terahertz metamaterials," *Nat Commun* **3**, 1151 (2012).
22. H. Ian, Y. X. Liu, and F. Nori, "Tunable electromagnetically induced transparency and absorption with dressed superconducting qubits," *Phys. Rev. A* **81**(6), 063823 (2010).
23. T. R. Zhan, X. Shi, Y. Y. Dai, X. H. Liu, and J. Zi, "Transfer matrix method for optics in graphene layers," *J. Phys. Condens. Matter* **25**(21), 215301 (2013).
24. A. Vakil and N. Engheta, "Transformation optics using graphene," *Science* **332**(6035), 1291–1294 (2011).
25. S. Thongrattanasiri, F. H. L. Koppens, and F. J. Garcia de Abajo, "Complete optical absorption in periodically patterned graphene," *Phys. Rev. Lett.* **108**(4), 047401 (2012).
26. Y. Lu, H. Xu, J. Y. Rhee, W. H. Jang, B. S. Ham, and Y. Lee, "Magnetic plasmon resonance: underlying route to plasmonic electromagnetically induced transparency in metamaterials," *Phys. Rev. B* **82**(19), 195112 (2010).
27. L. V. Hau, S. E. Harris, Z. Dutton, and C. H. Behroozi, "Light speed reduction to 17 metres per second in an ultracold atomic gas," *Nature* **397**(6720), 594–598 (1999).
28. U. Schnorrberger, J. D. Thompson, S. Trotzky, R. Pugatch, N. Davidson, S. Kuhr, and I. Bloch, "Electromagnetically induced transparency and light storage in an atomic Mott insulator," *Phys. Rev. Lett.* **103**(3), 033003 (2009).
29. M. F. Yanik, W. Suh, Z. Wang, and S. Fan, "Stopping light in a waveguide with an all-optical analog of electromagnetically induced transparency," *Phys. Rev. Lett.* **93**(23), 233903 (2004).

## 1. Introduction

Optical analogs of electrically induced transparency (EIT) in atomic systems have been proposed in a variety of optical structures [1–6]. One particularly interesting example is the plasmonic EIT in metal structures [3,7–10]. Involved radiative and dark modes typically have spatial sizes that are a few times smaller than the corresponding wavelengths in vacuum [3,8]. The strong spatial coupling between radiative and dark modes in such a subwavelength length scale may create a destructive interference between two different excitation channels, leading to a transparent window that is analogous to the atomic EIT.

Even being one-atomic-layer thick, graphene has shown many interesting optical properties in addition to appealing electronic, structural, and transport ones [11], largely due to the existence of plasmons [12–14]. As a result, graphene is manifest as a new class of plasmonic material in terahertz regime with important potential applications in photonics and optoelectronics [15,16]. Plasmons in a single graphene layer surrounded by two dielectrics can be approximately described by  $\omega = \sqrt{4\alpha c E_F k / \hbar(\epsilon_1 + \epsilon_2)}$  [12–14], where  $\omega$  is the angular frequency,  $k$  is the wave vector,  $E_F$  is the Fermi energy of the graphene layer,  $\alpha$  is the fine-structure constant,  $\hbar$  is the reduced Planck constant,  $c$  is the speed of light in vacuum, and  $\epsilon_1$  and  $\epsilon_2$  are the dielectric constants of the two dielectrics. Such a dispersion relation shows two unique features. First, it exhibits modal profiles with a deep-subwavelength confinement. For instance, for a plasmon mode with a frequency of 20 THz (corresponding to a wavelength of 15  $\mu\text{m}$  in vacuum) supported by a graphene layer in air the corresponding plasmon wavelength is smaller than 400 nm for  $E_F = 0.15$  eV. Such small modal sizes may open up new opportunities for engineering optical modes at a deep-subwavelength length scale.

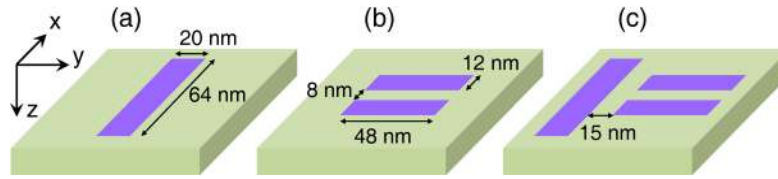


Fig. 1. Schematic view of graphene nanostructures under study. (a) A single graphene strip serving as the radiative element. (b) Two identical parallel graphene strips serving as the dark element. (c) The basic unit of the graphene plasmonic structure for achieving EIT which is a combination of the radiative (a) and dark (b) elements. Purple regions represent graphene and the shallow greenish layer stands for the supporting dielectric substrate

In this paper, we demonstrate numerically a plasmonic analog of the atomic EIT based on graphene nanostructures that can support plasmonic resonances with different optical properties. Compared with the plasmonic EIT in metal structures, our graphene-based EIT offers a much closer analogy to the atomic EIT in the sense of the deep-subwavelength nature. As is known, the frequencies of plasmons in graphene depend strongly on the Fermi energy which can be tuned through doping or electrostatic gating [17–20]. The demonstrated EIT in nanostructured graphene has thus two appealing features: the deep-subwavelength nature and tunability which are difficult to attain in conventional metal structures. Both features are highly desired, e.g., in slow-light applications [21,22].

## 2. Design of plasmonic modes

To demonstrate the EIT phenomenon based on graphene, we start by designing resonant plasmonic nanostructures with distinct radiation properties as shown schematically in Fig. 1: radiative and dark elements whose profiles are similar to those metallic plasmonic structures in [3]. As will be shown later, the resonant plasmonic modes in the radiative and dark elements have strong and weak coupling to free space, respectively. The radiative element that supports radiative modes is simply a single graphene strip with a dimension of 20 nm by 64 nm, lying along the  $x$  direction. The dark element for dark modes consists of two identical parallel graphene strips with a dimension of 12 nm by 48 nm, lying along the  $y$  direction. The separation between the two graphene strips is 8 nm. The basic unit of the graphene plasmonic structure for realizing EIT is a combination of the radiative and dark elements with a separation of 15 nm. This separation is a key parameter to control the coupling between the two modes. Large separations usually give rise to a weak coupling. All graphene nanostructures are situated on a supporting dielectric substrate with a dielectric constant of 2.1 and a thickness of 20 nm. Note that the resonant modes of the graphene nanostructures are also influenced by the dielectric constant of the substrate. This dependency on the substrate's dielectric constant may provide an additional degree of freedom to tailor the resonant modes.

All graphene plasmonic nanostructures are numerically studied using the finite integration package (CST Microwave Studio). A frequency-domain solver is used with unit-cell boundary conditions in the  $x$ – $y$  plane and Floquet ports in the  $z$  direction for terminating the domain. In the simulations, graphene is modeled by an ultrathin layer of electron gas whose conductivity is simply given by a Drude term [19,23], namely,  $\sigma(\omega) = i4\alpha\epsilon_0cE_F / \hbar(\omega + i/\tau)$ ,

where  $\epsilon_0$  is the vacuum permittivity and  $\tau$  is the intrinsic relaxation time, taken to be 1 ps. Graphene can thus be described effectively by a dielectric function  $\epsilon(\omega) = 1 + i\sigma / \omega\epsilon_0$ , where  $t$  is the thickness of the ultrathin layer of electron gas, taken to be 1 nm, similar to that used in [24].

## 3. Results and discussions

The radiative properties of the radiative and dark elements are numerically studied. As is known, doped or gated graphene can support propagating plasmons that are tightly bounded at graphene [12–14]. In graphene nanostructures such as strips and disks, however, plasmon modes become localized [19,20,25], similar to those in metallic structures. For the dark

element, i.e., a single graphene strip, it can be simply viewed as a dipole antenna since its dimension is much smaller than light wavelengths in vacuum. The resonant frequencies of the dipole antenna can be approximately estimated from the dispersion of graphene plasmons  $\omega(K)$ , where  $K = m\pi/L$  is the effective wave vector with  $L$  being the strip length and  $m$  the order of the dipole resonances [20]. This could offer a simple estimation of the strip length used for numerical simulations in order to find the desired resonant frequency. Indeed, from our numerical simulations the radiative element can support an electric dipole mode with a resonant frequency at 23.38 THz as shown in Fig. 2(a). It can be efficiently excited by an incident field with the electrical field polarized along the strip direction. Note that the geometrical dimension of the graphene strip (20 nm by 64 nm) is 200 times smaller than the corresponding resonant wavelength in vacuum (12.83  $\mu\text{m}$ ), implying a deep-subwavelength nature.

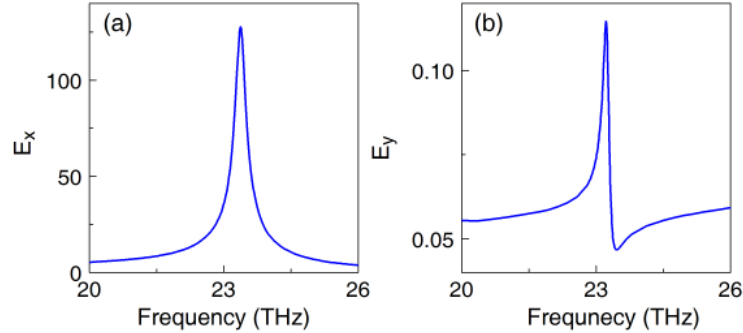


Fig. 2. Spectral response for (a) the radiative and (b) dark elements for  $E_F = 0.3$  eV. In (a), light with the electric field polarized along the  $x$  direction is incident normally to the surface. An  $E_x$  probe is placed 5 nm apart from the center of the end facet of the graphene strip. In (b), light with the electric field polarized along the  $y$  direction is incident at an incident angle of  $45^\circ$  to the surface normal. An  $E_y$  probe is placed 5 nm apart from the center of the end facet of one of the graphene strips.

The dark element, i.e., the pair of identical parallel graphene strips, can support symmetric and antisymmetrical localized plasmonic modes with different resonant frequencies. The geometrical parameters of the element are carefully chosen such that an antisymmetrical mode has a resonant frequency that is coincident with that of the dipole mode in the radiative element. In general, the plasmonic modes in the dark element cannot be excited by plane waves at normal incidence due to the lack of a direct electric dipole coupling [3]. However, they could be activated at oblique incidence as shown in Fig. 2(b) although the excitation efficiency is very low. By inspecting its field profiles, the antisymmetrical mode is basically an electric quadrupole mode in nature. Due to its very weak coupling to free space, this quadrupole mode can thus effectively act as a dark mode. Note that both the dipole and quadrupole modes may cause a phase difference between the localized electric and magnetic fields [26], which is essential for realizing EIT. In [21], metal split-ring resonators were used as the dark element to achieve plasmonic EIT. In principle, we could also adopt such splitting nanostructures made of graphene. One difference is that the dark mode in graphene splitting resonators is a magnetic resonance.

To observe the plasmonic EIT phenomenon in nanostructured graphene, we construct a graphene EIT structure by using the basic unit consisting of the coupled radiative and dark elements [Fig. 1(c)] as building blocks. The units occupy periodically the entire substrate in a square lattice with a period of 120 nm. Near-field couplings between neighboring units can be neglected due to the deep-subwavelength confinement of plasmonic resonances in graphene nanostructures. With such a construction, there are no diffractions for THz light due to the small periodicity. The simulated transmission and reflection spectra for the graphene EIT structure under normal incidence are shown in Fig. 3.

Obviously, the transmission spectrum of the graphene EIT structure shows an EIT-like transparent window with a peak frequency of 23.25 THz in addition to two dips positioned at 22.93 and 23.63 THz, which is basically similar to the EIT spectrum in atomic systems. At the EIT transparent window, there is nearly no reflection. At the transmission dips, the reflection is still very small, indicating a large absorption. To visualize the interference between the dark and radiative modes, we also show the distributions of the electric field  $|\mathbf{E}|$  at these interested frequencies. For the transparent peak at 23.25 THz, incident light can directly excite the dipole mode in the radiative element while the direct excitation of the quadruple mode in the dark element is not allowed. However, the dark mode can be indirectly excited via the coupling between the radiative and dark modes. The indirectly excited dark mode will then couple back to the radiative mode. Note that there exists a phase difference of  $\pi$  between the channels of the direct and indirect excitations [3,26]. As a result, the radiative and dark modes interfere destructively with each other, and in the meantime the fields in the radiative element are suppressed, eventually leading to a transparent window, analogous to the atomic EIT. In contrast, at the transmission dips the interference is constructive such that the fields in both elements are enhanced.

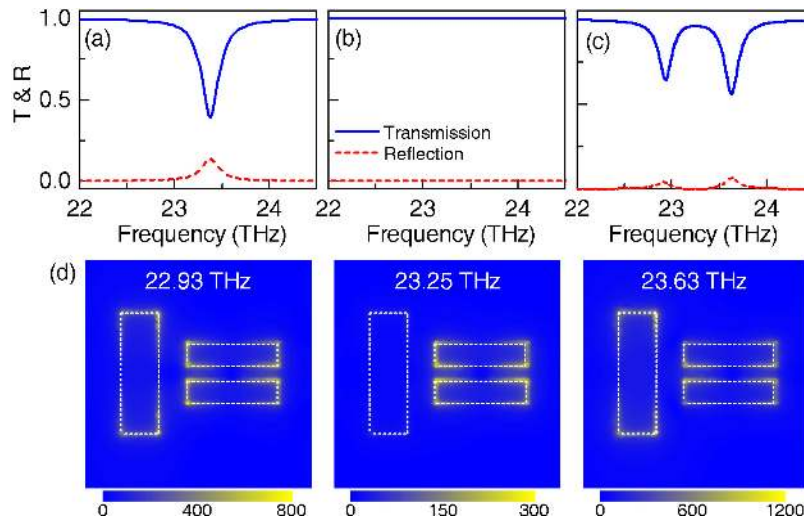


Fig. 3. Transmission and reflection spectra under normal incidence for the basic unit containing (a) the radiative element, (b) the dark element, and (c) the EIT unit, i.e., the coupled radiative-dark element with  $E_F = 0.3$  eV. Incident light is polarized along the direction of the long axis of the radiative element. (d) Distributions of the electric field  $|\mathbf{E}|$  at the interface between the graphene EIT structure and the supporting substrate for three different frequencies. Graphene strips are outlined by white dashed lines.

Optical properties of graphene can be substantially modified via doping or gating since plasmons in graphene depend strongly on the Fermi energy [12–14]. By tuning the Fermi energy, the electron density in graphene is changed, resulting in the change of the resonance frequencies of graphene plasmonic nanostructures [17]. Therefore, we can dynamically control the EIT spectrum of the graphene EIT structure over a broad range of frequencies. Note that such tunability is difficult to accomplish in atomic or other EIT systems. Figure 4(a) shows the transmission spectra for the same graphene EIT structure but at different  $E_F$ . Obviously, the center frequency of the EIT transparency window can shift from 18.84 to 26.94 THz with  $E_F$  varying from 0.2 to 0.4 eV.

EIT has been demonstrated to be able to greatly slow down the speed of light [27,28]. Slow light is important for routing optical information. In particular, it is highly desired that slow light can be achieved on-demand and with flexibility for tuning [1,29]. The EIT phenomena demonstrated in graphene plasmonics offers a unique capability for electrical tuning. In Fig. 4(b), we show the group delays for the graphene EIT structure at different  $E_F$ .

Positive and negative group delays correspond to slow and fast light, respectively. Obviously, in the vicinity of the EIT transparent peak it offers large positive group delays, suggesting slow light. At the transparent peak, the group delays for different  $E_F$  are more than 0.04 ps, equivalently corresponding to a distance of 12  $\mu\text{m}$  for light traveling in vacuum. Considering graphene is only one-atomic-layer thick (1 nm in our simulations) and the substrate is 20-nm thick, in the vicinity of the transparent peak the effective group refractive index of the graphene EIT structure should be more than 500, one order of magnitude larger than that offered by the plasmonic EIT in metal structures [3]. Moreover, by tuning the Fermi energy one can shift the EIT spectrum over a fairly wide range of frequency. Therefore, we can achieve the capability of turning on and off the group delay and controlling the amount of the group delay by tuning the Fermi energy.

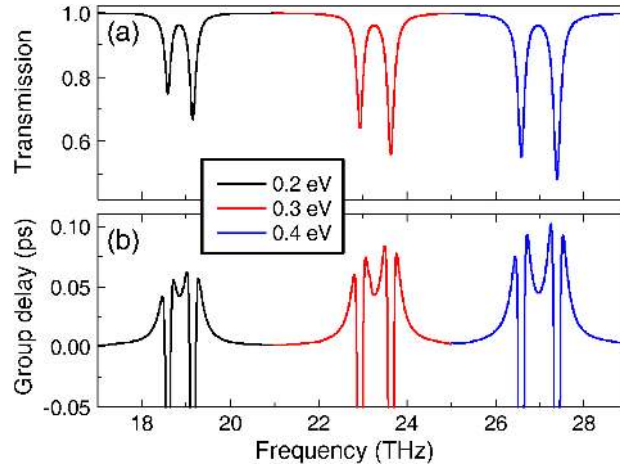


Fig. 4. (a) Transmission spectra of the graphene EIT structure under normal incidence at different  $E_F$ . (b) Corresponding group delays.

#### 4. Conclusion

In conclusion, by numerical simulations we study the radiative properties of graphene nanostructures. These graphene nanostructures can support plasmonic resonant modes with deep-subwavelength modal profiles. In particular, a graphene strip can serve as the radiative element while two identical parallel graphene strips can act as the dark element. By using the coupled radiative and dark elements as building blocks, a graphene EIT structure is constructed showing an EIT spectrum that is closely analogous to the atomic EIT. Compared with plasmonic EIT in metal structures, the graphene EIT manifests a closer analog to atomic systems in the sense of the deep-subwavelength nature. Importantly, the EIT spectrum can be tuned electrically by applying a gate voltage. Moreover, the graphene EIT structure can offer extremely large group delays, one order of magnitude larger than those offered by metal structures. These promising features could lead to new opportunities for applications in the terahertz regime, e.g., in slow light, spectral filtering, and sensing.

#### Acknowledgments

This work is supported by the 973 Program (Grant Nos. 2013CB632701 and 2011CB922004). The research of H.C., X.H.L., and J.Z. is further supported by the National Natural Science Foundation of China.